JOURNAL OF AGRICULTURAL AND FOOD CHEMISTRY
ARTICLE

J. Agric. Food Chem. 2010, 58, 11993–11999 11993
DOI:10.1021/jf102763p

Physical Structures in Soybean Oil and Their Impact on Lipid Oxidation

Bingcan Chen, Ashley Han, David Julian McClements, and Eric Andrew Decker*

Department of Food Science, University of Massachusetts, Amherst, Massachusetts 01003, United States

The oxidation of edible oil yields both primary and secondary oxidation products (e.g., hydroperoxides, carbonyls, hydrocarbons, and epoxides), which produce undesirable sensory and biological effects. Consequently, the suppression of lipid oxidation in food matrices is of great importance. The rate and extent of lipid oxidation in many heterogeneous foods are strongly affected by the physicochemical characteristics of water−oil interfaces. This study examined the ability of dioleoylphosphatidylcholine (DOPC) and water to form association colloids within bulk oil, as well as their impact on lipid oxidation kinetics. Attenuation was used to show the DOPC and water concentrations at which association colloids existed without altering the optical properties of the oil. Interfacial tension and fluorescence spectrometry showed the critical micelle concentration (CMC) of DOPC in stripped soybean oil was around 650 μM at room temperature. Small-angle X-ray scattering (SAXS) and fluorescence probes showed that water had a very strong impact on the properties of the association colloids formed by DOPC. Measurement of primary and secondary lipid oxidation products revealed that the association colloids formed by DOPC had a pro-oxidant effect. The characterization of association colloids could provide a better understanding of the mechanisms of lipid oxidation in bulk oils and provide insights into new antioxidant technologies.

KEYWORDS: Lipid oxidation; phospholipids; bulk oil; association colloids; reverse micelles

INTRODUCTION

Bulk oil is often assumed to be a homogeneous liquid, in contrast to more complex multiphase systems, such as emulsions, which are regarded as heterogeneous liquids. However, refined oil, which is processed to remove many of the non-triacylglycerol fractions, still contains numerous minor components that are amphiphilic, such as monoacylglycerols, diacylglycerols, phospholipids, sterols, free fatty acids, and polar products arising from lipid oxidation, such as lipid hydroperoxides, aldehydes, ketones, and epoxides (*1*−*3*). In addition, refined oils also contain small but significant amounts of water. Previous studies have demonstrated that surface active molecules can self-assemble in the presence of water to form a variety of association colloids in nonpolar solvents (e.g., benzene, isooctane, cyclohexane, toluene, free fatty acids, and triacylglycerols), such as reverse micelles, microemulsions, lamella structures, and cylindrical aggregates (*4*−*6*). For instance, Sosaku and co-workers formed reverse micelle systems using soybean phospholipids as a surfactant in fatty acid or fatty acid ethyl esters as the organic solvent (*7*). Sinoj and co-workers recently formed nutrient delivery systems consisting of water-in-oil nanoemulsions using oleic acid embedded in canola oil (*8*). These studies suggest that the amphiphilic molecules in refined vegetable oils have the ability to form association colloids (*9*).

The mechanism of lipid oxidation in bulk oil has been studied for decades (*10*). Research over the past two decades has shown that in emulsion systems, lipid oxidation is strongly influenced by the physical properties of the emulsion droplets and their interfaces, which can affect pro-oxidant/lipid interactions and the location of antioxidants (*11*). Most previous research has treated bulk oils as homogeneous systems without considering how lipid oxidation reactions could be influenced by their physical structures. If bulk oils are actually microheterogeneous systems containing association colloids, it is highly likely that these physical structures will affect lipid oxidation as they do in emulsion systems.

To better understand how microstructures affect the oxidation of bulk oil, it will be necessary to develop model association colloid systems that reflect the types of physical structures that would be expected to exist in refined vegetable oils. Therefore, in this study, a model system consisting of different concentrations and types of phospholipids [1,2-dioleoyl-*sn*-glycero-3-phosphocholine (DOPC) and 1,2-dibutyryl-*sn*-glycero-3-phosphocholine (DC_4PC), **Figure 1**] and water was used to characterize association colloids in stripped soybean oil and to evaluate their impact on lipid oxidation.

MATERIALS AND METHODS

Materials. Avanti Polar Lipids, Inc. (Alabaster, AL) was the source of 1,2-dioleoyl-*sn*-glycero-3-phosphocholine (DOPC) and 1,2-dibutyryl-*sn*-glycero-3-phosphocholine (DC_4PC). *N*-(7-Nitrobenz-2-oxa-1,3-diazol-4-yl)-1,2-dihexadecanoyl-*sn*-glycero-3-phosphoethanolamine, triethylammonium salt (NBD-PE), was acquired from Invitrogen (Carlsbad, CA). Soybean oil was purchased from a local store and stored at 4 °C. Silicic acid (100−200 mesh), activated charcoal (100−400 mesh), 7,7,8,8-tetracyanoquinodimethane (7,7,8,8-TCNQ), and hexane were purchased from Sigma-Aldrich Co. (St. Louis, MO). Medium-chain triacylglycerols (MCT, Miglyol) were purchased from Sasol North America Inc. (Houston, TX). All other reagents

*Author to whom correspondence should be addressed [phone (413) 545-1026; fax (413) 545-1262; e-mail edecker@foodsci.umass.edu].

Published on Web 10/22/2010

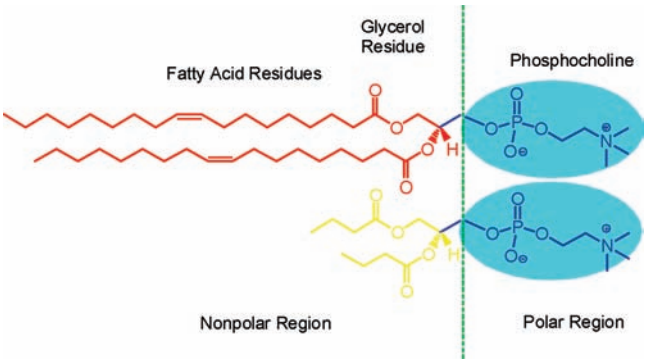

Figure 1. Molecular structures of 1,2-dioleoyl-*sn*-glycero-3-phosphocholine (DOPC) and 1,2-dibutyryl-*sn*-glycero-3-phosphocholine (DC_4PC).

were of HPLC grade or purer. Distilled and deionized water was used in all experiments.

Preparation of Stripped Soybean Oil. Stripped soybean oil (SSO) was prepared according to the method of Boon et al. (*12*). In short, silicic acid (100 g) was washed three times with a total of 3 L of distilled water and activated at 110 °C for 20 h. Activated silicic acid (22.5 g) and activated charcoal (5.625 g) were suspended in 100 and 70 mL of *n*-hexane, respectively. A chromatographic column (3.0 cm idnternal diameter × 35 cm height) was then packed sequentially with 22.5 g of silicic acid followed by 5.625 g of activated charcoal and then another 22.5 g of silicic acid. Thirty grams of soybean oil was dissolved in 30 mL of hexane, which was then loaded onto the column and eluted with 270 mL of *n*-hexane. To retard lipid oxidation during stripping, the collected soybean oil was held on ice and covered with aluminum foil. The solvent in the stripped oil was removed with a vacuum rotary evaporator (RE 111 Buchi, Flawil, Switzerland) at 37 °C, and the remaining trace solvent was removed by flushing with nitrogen for at least 1 h. The colorless stripped oil was kept at −80 °C for subsequent studies. Removal of minor components was verified by spotting a sample on a silica gel G thin layer chromatography (TLC) plate, developed in a tank with hexane/diethyl ether/acetic acid (70:30:1 v/v/v), and separated compounds were detected by sulfuric acid charring (*13*). The water content of the stripped oils was determined by Karl Fisher (*14*).

Light Scattering Properties of Oil Samples. A series of samples were prepared to determine the DOPC and water concentrations that produced association colloids without causing cloudiness in the oil. A stock solution of DOPC was prepared at a concentration of 127 μmol of DOPC/mL of chloroform, which was blended into MCT over the concentration range of 0−1270 μmol/kg of lipid, which is in the range of phospholipid concentrations found in refined bulk oils (~2000 μmol/kg of lipid). The mixture of MCT and DOPC was then titrated with water. The initial water concentration in the samples was 0.67 mmol/kg of lipid (determined by Karl Fisher analysis) and was increased to 560 mmol/kg of lipid by adding water. The vials were tightly closed with Teflon-lined caps and placed on a stirrer motor at 25 °C for 24 h before measurements. The final water concentrations were verified by Karl Fisher analysis. The clarity of the samples was measured by light scattering using an Agilent 7010 particle size spectrophotometer. The Agilent 7010 particle size spectrophotometer measures the attenuation of a colloidal dispersion from 350 to 800 nm. The transparent region was defined as samples with a measured attenuation of ≤ 0.2 cm^{-1} (visibly clear), whereas the cloudy region was defined as samples with attenuation of > 0.2 cm^{-1}.

Determination of Critical Micelle Concentration (CMC) in Stripped Soybean Oil. The procedure described by Kanamoto and coworkers (*15*) was followed to spectrophotometrically determine the CMC of the phospholipids in SSO. In short, various concentrations of DOPC or DC_4PC were dissolved in either SSO or MCT by mixing for 12 h followed by addition of 7,7,8,8-TCNQ (5 mg) to 5 g of oil/DOPC in a small conical flask, and the mixture was agitated using a magnetic stirrer for 5 h at room temperature. After sedimentation of excess TCNQ by centrifugation at 2000*g* for 20 min, absorbance measurements at 480 nm were recorded (Shimadzu 2014, Tokyo, Japan). SSO or MCT without DOPC was used as control. The CMC was taken as the intersection point of straight lines extrapolated from low and high DOPC concentrations in the curve generated from absorbance and DOPC concentrations on a semilog plot.

The CMC of DOPC in SSO was also determined by interfacial tension (IFT) measurements using Drop Shape Analysis (DSA100, Krüss GmbH, Hamburg, Germany) equipped with a pendant drop module. A needle with a diameter of 1.830×10^{-3} m was used to create a pendent drop (containing the SSO and various concentrations of DOPC). The pendant drop was extruded from the syringe into a quartz cell containing distilled water. Droplet images were taken every 2 s, and the drop shape analysis program supplied by the instrument manufacturer (based on the Young−Laplace equation) was used to determine IFT values.

Small-Angle X-ray Scattering (SAXS). SAXS measurements were performed on the oil samples containing various concentrations of phospholipids and water using a Rigaku Molecular Metrology SAXS instrument (Rigaku, Inc.) at the W. M. Keck Nanostructures Laboratory at the University of Massachusetts—Amherst. The instrument generates X-rays with a wavelength of 1.54 Å and utilizes a 2-D multiwire detector with a sample-to-detector distance of 1.5 m. Samples were inserted into the 1 mm outer diameter quartz capillary (Hampton Research, Aliso Viejo, CA), which was then sealed by Duco Cement and then enclosed in an airtight sample holder. This assembly was then put in the X-ray beam path, and data were collected on the samples for 3 h.

The experimental SAXS intensity curves were corrected for background, sample absorption, and detector homogeneity, using MicroCal Origin 5.0 software. The scattering vector amplitude q is defined by eq 1, where θ is half of the scattering angle and λ is the wavelength:

$$q = 4\pi\frac{\sin\theta}{\lambda} \quad (1)$$

Fittings for the experimental SAXS curves were obtained using the GNOM program (version 4.5, ATSAS, Germany) (*16*). For a set of monodisperse spherical particles randomly distributed, the scattering intensity is given by the equation (*17*)

$$I(q) = \gamma n_p(\Delta\rho)^2 V^2 P(q) S(q) \quad (2)$$

where γ is a factor related to the instrumental effects, n_p corresponds to the number of scattering species, $\Delta\rho$ is the electron density contrast between the scattering species and the medium, V is the scattering species volume, P is the normalized particle form factor [$P(0) = 1$], and S is the structure factor of the particle system, its value being ≈1 for noncorrelated systems. In this particular case, the intensity function I depends solely on the particle form factor, and according to theory, the pair-distance distribution function $p(r)$ can be obtained by Fourier inversion of the intensity function (*18*):

$$p(r) = \frac{1}{2\pi^2}\int_0^1 I(q) qr \sin(qr)\, dq \quad (3)$$

This function provides information about the shape of the scattering particles as well as their maximum dimension, D_{max}, accounted for by the r (pair distance) value where $p(r)$ goes to zero.

Front-Face (FF) Fluorometric Measurements. Front-face fluorescence with surface active fluorescent probes was used to verify the ability of DOPC and water to form association colloids. The surface active fluorescent probe used was NBD-PE, which is a phospholipid analogue with a fluorescent functional group covalently attached to the choline headgroup. Steady-state emission measurements were recorded with a PTI spectrofluorometer (PTI, Ontario, Canada) with the sample holder held at 22 °C. To minimize any reflection of the excitation beam by the cell window and by the underlying liquid surface of the sample into the emission monochromator, samples were stored in triangular suprasil cuvettes. The emission was observed at 90° to the incident beam, that is, 22.5° with respect to the illuminated cell surface. A 2.0 nm spectral bandwidth for both excitation and emission slits was employed for the NBD-PE excitation at 468 nm. The integration time was 1 s, and the wavelength increment during emission spectrum scanning was 1 nm. The intensity of the spectra was determined as the emission signal intensity (counts per second) measured by means of a photomultiplier. To avoid self-quenching of probes, the concentration of NBD-PE was 9.5 μM ($^1/_{100}$ of DOPC) (*19*).

Measurement of Oxidation Parameters. Lipid hydroperoxides were measured as the primary oxidation product using a method adapted from

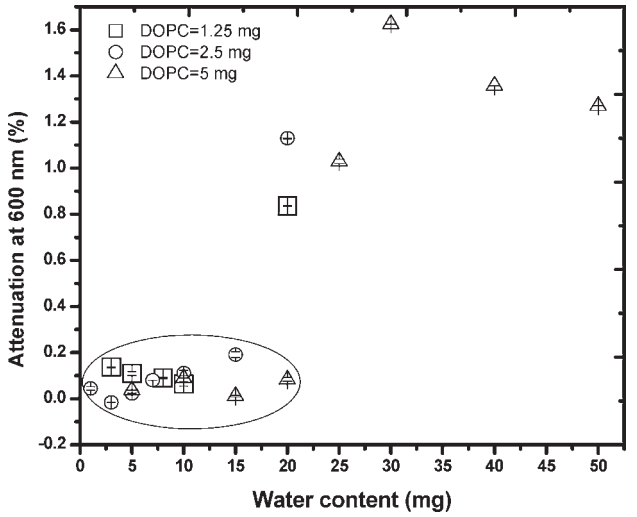

Figure 2. Attenuation of medium-chain triacylglycerol (MCT) samples containing 1,2-dioleoyl-*sn*-glycero-3-phosphocholine (DOPC) and various concentrations of water.

Shanta and Decker (*20*). Accurately weighed oil samples were added to a mixture of methanol/butanol (2.8 mL, 2:1, v/v) followed by the addition of 15 μL of 3.94 M thiocyanate and 15 μL of 0.072 M Fe^{2+} (ferrous sulfate). The solution was vortexed, and after 20 min, the absorbance was measured at 510 nm using a Genesys 20 spectrophotometer (ThermoSpectronic, Waltham, MA). The concentration of hydroperoxides was calculated from a cumene hydroperoxide standard curve.

Secondary oxidation products were monitored using a GC-17A Shimadzu gas chromatograph equipped with an AOC-5000 autosampler (Shimadzu, Kyoto, Japan) (*21*). Samples (1 mL) in 10 mL glass vials capped with aluminum caps with PTFE/silicone septa were preheated at 55 °C for 15 min in an autosampler heating block. A 50/30 μm DVB/Carboxen/PDMS solid-phase microextraction (SPME) fiber needle from Supelco (Bellefonte, PA) was injected into the vial for 2 min to absorb volatiles and then was transferred to the injector port (250 °C) for 3 min. The injection port was operated in split mode, and the split ratio was set at 1:5. Volatiles were separated on a Supleco 30 m × 0.32 mm Equity DB-1 column with a 1 μm film thickness at 65 °C for 10 min. The carrier gas was helium at 15.0 mL/min. A flame ionization detector was used at a temperature of 250 °C. Propanal concentrations were determined from peak areas using a standard curve prepared from an authentic standard.

Statistical Analysis. Duplicate experiments were performed for all studies. All data shown represent mean values ± standard deviations ($n = 3$). A significance level of $p < 0.05$ between groups was accepted as being statistically different. In all cases, comparisons of the means of the individual groups were performed using Duncan's multiple-range tests. All calculations were performed using SPSS17 (http://www.spss.com; SPSS Inc., Chicago, IL).

RESULTS AND DISCUSSION

Attenuation of the Water/Phospholipid/MCT System. Commercial refined vegetable oils are optically clear and yet potentially contain physical structures such as association colloids. This is possible because many association colloids have dimensions below 100 nm, and thus they do not strongly scatter visible light (*22*). The objective of this initial study was to define the phospholipid/water/lipid concentrations that produce optically transparent oils, corresponding to commercial refined oils. To do this, a partial phase diagram of the three-component system water/phospholipid/MCT was constructed to determine the phospholipid and water concentrations that did not form structures that scattered light strongly as determined by light attenuation measurements (**Figure 2**) using a method previously reported for phospholipids and water in olive oil (*23*). In the presence of 1.25, 2.5, and 5 mg DOPC/g MCT, a large increase in attenuation was observed at a water concentration of ≥20 mg/g MCT. At 20 mg/g MCT, the attenuation of the sample containing the highest concentration of DOPC (5 mg DOPC/g MCT) had the lowest attenuation. This is likely due to the formation of a larger number of small non-light-scattering association colloids in the presence of high levels of DOPC. In the remainder of the experiments we focused on those phospholipid/water/lipid concentrations that gave optically transparent systems.

Determination of the CMC of Phospholipids in SSO and MCT. Phospholipids can self-assemble into a variety of structures in water or oil phases because of their amphiphilic nature (*24*). The nature of the structures formed depends on the phospholipid's chemical structure and solvent type (*25*). In nonaqueous media, such as oil, phospholipids normally form reverse micelles when their concentration just exceeds the CMC, with the polar headgroups pointing into the hydrophilic core of the reverse micelle and the nonpolar tails pointing toward the hydrophobic oil. Therefore, in the region of the phase diagram where the system is clear (**Figure 2**), it is important to determine whether the DOPC concentration is above or below its CMC so as to determine if any association colloid structures form. SSO can rapidly oxidize, resulting in the production of additional surface active oxidation products, which could alter the CMC. Therefore, the CMC of DOPC was measured in both SSO and MCT to determine if SSO was a suitable solvent for the analysis of association colloids.

One of the most important properties of reverse micelles is their ability to increase the solubility of molecules. 7,7,8,8-TCNQ is not lipid soluble and does not absorb light at 480 nm when dispersed in nonpolar solvents. 7,7,8,8-TCNQ can undergo charge-transfer (*4*) interactions with surfactants when the surfactant concentration is above the CMC, which can be observed by absorbance at 480 nm (*15*). The absorbance values of 7,7,8,8-TCNQ solubilized in MCT were plotted as a logarithmic function of phospholipid concentration (**Figure 3A**). When the concentration of DOPC was increased, the absorbance of TCNQ initially remained low, but there was a rapid increase in absorbance at DOPC concentrations above 500 μM ($p \leq 0.05$). On the basis of the intercept of these two linear regions, the CMC of DOPC was estimated to be ~550 μM in MCT. This experiment was repeated in SSO, where the CMC of DOPC was found to be ~650 μM (**Figure 3B**). Differences of the CMC in MCT and SSO could be due to differences in fatty acid chain length and the presence of other minor surface active components in the oils that were not completely removed by stripping (*26*). Because the CMC values for MCT and SSO were fairly similar, SSO was used for all subsequent experiments. The CMC of DC_4PC in the SSO could not be determined by this method because DC_4PC did not dramatically change the absorbance of the 7,7,8,8-TCNQ before the DC_4PC reached its solubility limit in the SSO.

The CMC of DOPC in SSO was also determined by interfacial tension measurements. At low DOPC concentrations, the interfacial tension decreased with increasing DOPC concentration, but at higher DOPC concentrations the interfacial tension reached a fairly constant value, indicating that reverse micelles had been formed. A semilogarithmic plot between interfacial tension and the concentration of DOPC in SSO is shown in **Figure 4**. On the basis of the intercept of the two linear regions, a CMC of ~950 μM was calculated. The CMC value obtained by interfacial tension measurements is about 300 μM higher than that obtained with the spectrophotometric technique, which could be due to some of the DOPC partitioning into the aqueous phase during the interfacial tension measurements. Alternatively, the spectrophotometric and interfacial tension methods may have given different CMC values because they are based on different physical principles. For the purposes of this study, we considered

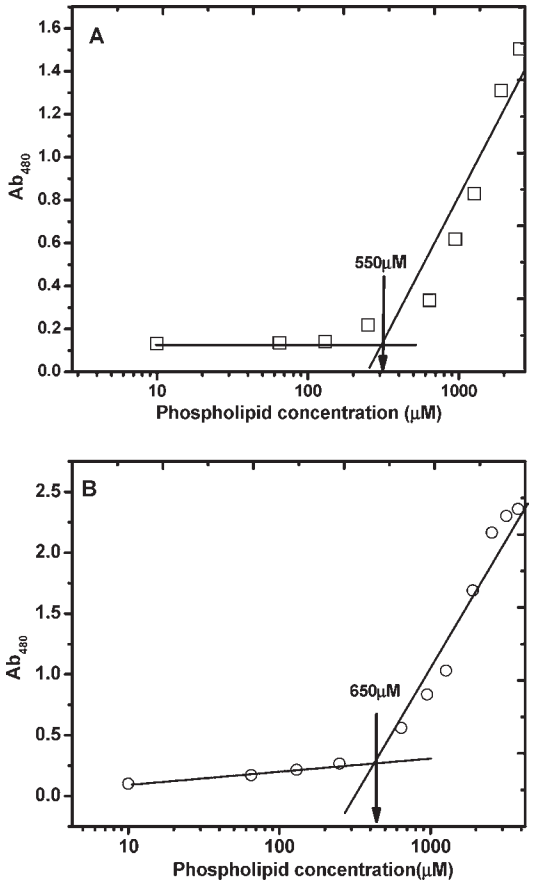

Figure 3. Determination of critical micelle concentration (CMC) of 1,2-dioleoyl-*sn*-glycero-3-phosphocholine (DOPC) in medium-chain triacylglycerols (**A**) and stripped soybean oil (**B**) as determined by the absorbance (480 nm) of 7,7,8,8-tetracyanoquinodimethane.

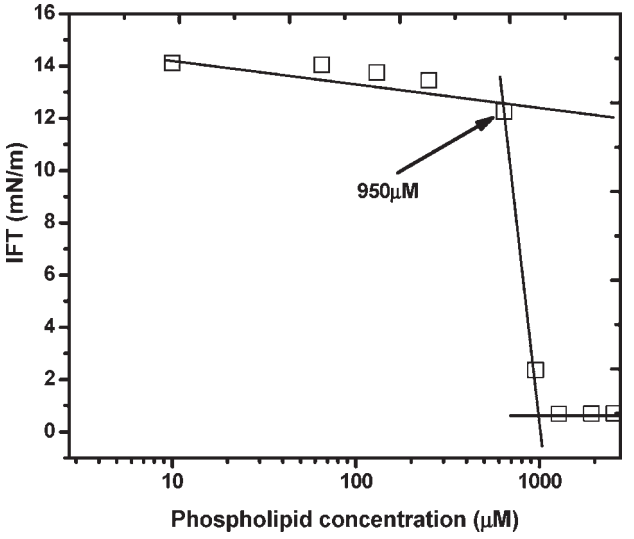

Figure 4. Determination of critical micelle concentration of 1,2-dioleoyl-*sn*-glycero-3-phosphocholine in stripped soybean oil using interfacial tension.

the CMC of DOPC in SSO to be in the range of 650−950 μM. The normal concentration of phospholipids in refined vegetable oil is > 950 μM, suggesting that commercial oils could have association colloids formed by phospholipids.

Detection and Characterization of Phospholipids Physical Structures by SAXS. As mentioned above, the specific structures formed by phospholipids in nonaqueous solution depend on both concentration and phospholipid type. In consideration of the complicated compositions of phospholipids in refined bulk oil, we first determined how two types of phospholipids affected association colloid structure in ternary systems containing SSO, water, and either DOPC or DC_4PC. **Figure 5** shows the SAXS profiles in the SSO systems containing ~60 ppm water (i.e., intrinsic water content after oil stripping) and 950 μM DOPC or DC_4PC. These phospholipid concentrations were chosen as these samples did not strongly scatter light (**Figure 2**) but were equal to or above the CMC of DOPC (**Figures 3** and **4**). As shown in **Figure 5**, the two different types of phospholipids induced changes of the minor structures in stripped oil in such a way that the scattering profiles are distinct and displaced toward different q values and intensity. The Bragg space (d-spacing) and the intensity of the samples with DOPC were similar to those of blank stripped oil, being 141 Å and 3 au, respectively. However, the structures with DC_4PC are quite different from the blank and the one with DOPC. Its Bragg peak shifts toward a higher q value with Bragg space being 68 Å, whereas the intensity rises to 12 (au). In addition, the structures with different types of phospholipids are verified by pair distribution $p(r)$ function analysis (**Figure 6**). The $p(r)$ of DC_4PC had a long tail at high r, which is typical of a cylindrical structure (*27*). The r value at the inflection (~20 nm) usually represents the diameter of the cylinder (*28*). The $p(r)$ of DOPC had a symmetrical shape, which represents a spherical structure, presumably a reverse micelle. For the bulk SSO, there was only a flat line indicating the presence of no structures.

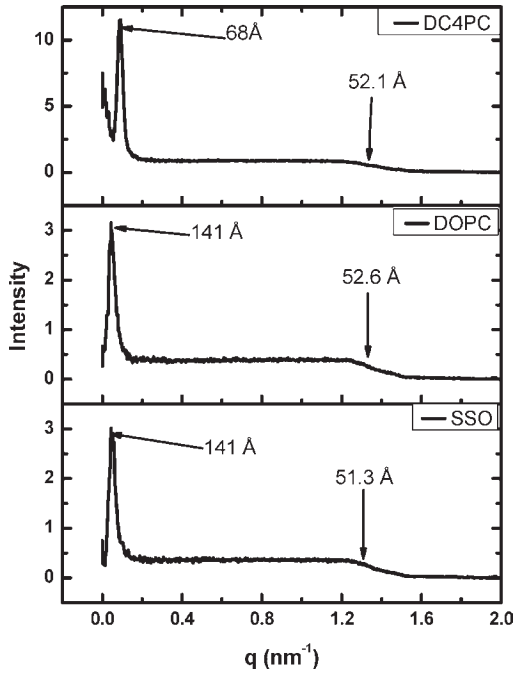

Figure 5. Small-angle X-ray scattering profiles of stripped soybean oil (SSO) and SSO + 950 μM 1,2-dioleoyl-*sn*-glycero-3-phosphocholine (DOPC) or 1,2-dibutyryl-*sn*-glycero-3-phosphocholine (DC_4PC).

In the stripped oil, almost all of the surface active minor components and the majority of water had been removed by the silicic acid and activated charcoal sandwich column chromatography, which is consistent to our, Karl Fisher, TLC, and previous HPLC results (*29*). Therefore, it is reasonable that the bulk stripped oil did not contain any association colloid structures (*30*). The structures formed by DC_4PC are quite different from those formed by DOPC. DOPC and DC_4PC have the same phosphocholine hydrophilic headgroup (**Figure 1**), but DOCP possesses *cis*-oleic fatty acids on *sn*-1 and *sn*-2 of the glycerol side

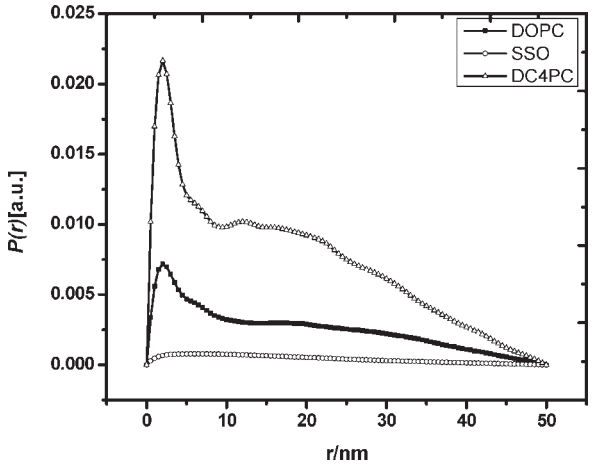

Figure 6. Pair distribution functions, $p(r)$, calculated from the scattering profiles of stripped soybean oil (SSO) and SSO + 950 μM 1,2-dioleoyl-*sn*-glycero-3-phosphocholine (DOPC) or 1,2-dibutyryl-*sn*-glycero-3-phosphocholine (DC_4PC) using GNOM analysis of the three small-angle X-ray scattering profiles indicated in **Figure 5**.

chains, whereas DC_4PC has two butyl fatty acids. As indicated, amphiphilic molecules, such as phospholipids, having a large tail area and a small headgroup area, can self-assemble into reverse spherical micelles in highly nonpolar liquids due to critical packing parameter (CPP) values of >1 (*31*). There are no reported CPP values of DC_4PC. However, on the basis of the CPP equation (*32*)

$$\mathrm{CPP} = \frac{\mathrm{V}}{\sum_0 l_c} \tag{4}$$

$$v\,(\text{Å}^3) = 27.4 + 26.9n \tag{5}$$

$$l_c\,(\text{Å}^3) = 1.5 + 1.265n \tag{6}$$

where v is the volume of the hydrocarbon tail and n is the number of carbons in the hydrophobic chain, the CPP of DC_4PC in SSO should be lower than that of DOPC, approximately less than half, assuming no difference of their effective area of the headgroup. This is because the CPP is mainly dependent on the hydrocarbon tail length. A low CPP often corresponds to the formation of cylindrical structures.

Effect of Water/Phospholipid Molar Ratio on the Physical Properties of DOPC Association Colloids. Experimental and theoretical approaches have shown that the key structural parameter of reverse micelles is the water/surfactant molar ratio (W_0) (*33*, *34*). On the one hand, water will serve to bridge the phosphate headgroups between neighboring phospholipids through hydrogen bonds (*35*). On the other hand, the water content will determine structure size as well as the amount of water that is strongly associated with the phospholipid headgroups (*19*). Oil-rich phospholipid solutions with micellar morphology can change to lamellar and hexagonal structures as the W_0 is raised in the system (*24*). To characterize the physical structure of SSO with DOPC (950 μM) as a function of W_0, a combination of SAXS and front-face fluorometry was used.

At high W_0, water is solubilized into phospholipid reverse micelles, and structures such as cylindrical micelles and spherical swollen micelles can form depending upon the amount of water in the system (*32*). In our system there is a clear Bragg peak on all of

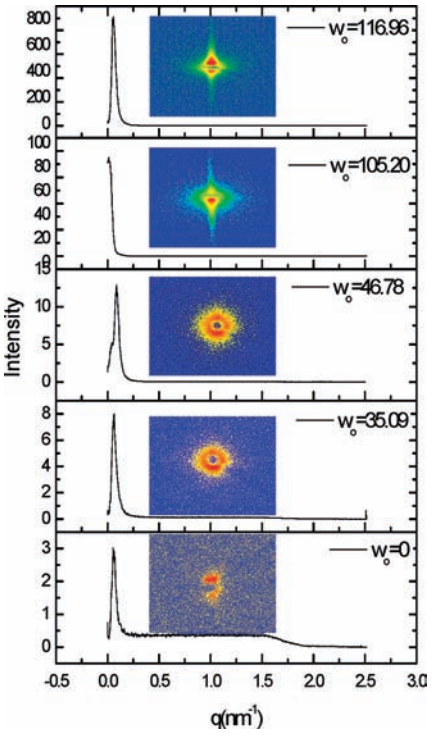

Figure 7. Small-angle X-ray scattering profiles of stripped soybean oil with different water/1,2-dioleoyl-*sn*-glycero-3-phosphocholine molar ratios (W_o). Insets are the two-dimensional small-angle X-ray scattering pattern of each sample.

the SAXS profiles, with *d*-spacing around 141 nm (**Figure 7**). The SAXS intensity is very weak (i.e., 3 au) for the system with $W_0 = 0$ (no added water), suggesting that DOPC alone forms very little structure. When the W_0 increased from 0 to 35 and 47, the scattering intensity increased from 3.0 to 8.0 and 13.0, respectively, presumably due to the formation of association colloids by DOPC. Increasing W_0 above 100 results in the 2-D X-ray pattern of the samples becoming aligned, indicating a transformation from an isotropic to an anisotropic system. At the same time, the SAXS intensity increased greatly to 749.6 au. In all samples, no other Bragg peaks were observed (**Figure 7**), indicating the absence of cylindrical micelles and spherical swollen micelles. Lack of transformation from reverse micelles to cylindrical micelles and spherical swollen micelles was also reported in a phospholipid in hexane and soybean oil system (*36*). The fact that the reverse micelles did not transform to these other colloidal structures in our system could be due to (1) the increase in W_0 being too small in our experimental design so that the transformation did not occur or (2) the concentration of the DOPC being too low to allow transformation. The anistropic transition at W_0 values of >100 indicates that the structures were changing symmetry. This could be due to a stretching of the symmetrical structure into more of a oblong structure such as shown in **Figure 8**.

The fluorescence intensity of selected probes can also be used to provide information about the microenvironment of association colloids as a function of W_0. In this study, we used NBD-PE as a fluorescence probe and front-face fluorometry to detect changes in its spectra. This probe is a phospholipid analogue grafted with a fluorophore on the phosphate headgroups (**Figure 9**, inset) that has previously been used as an indicator of changes in the interfacial properties of reverse micelle systems (*19*). Theoretically, NBD-PE possesses properties similar to those of DOPC as both are amphiphilic molecules with the ability to participate in the formation of association colloids and reside at the water−oil

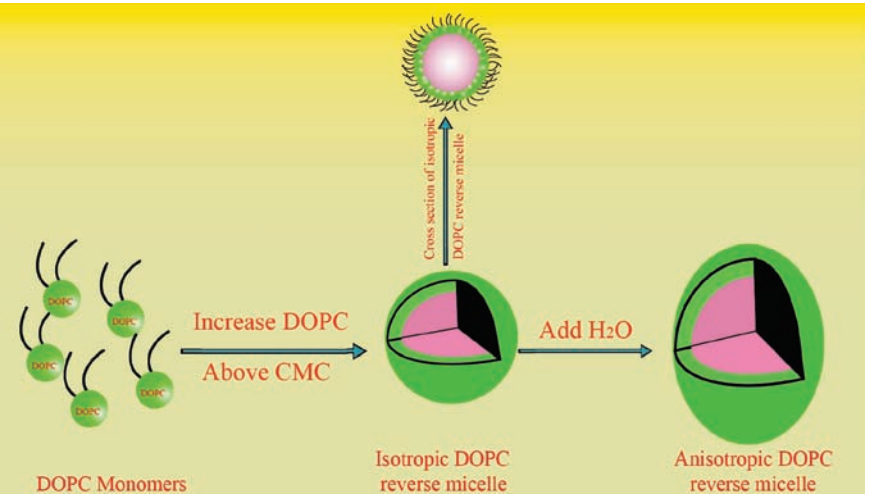

Figure 8. Postulated structural change of 1,2-dioleoyl-*sn*-glycero-3-phosphocholine (DOPC) as phospholipid concentrations are increased to above the critical micelle concentrations (CMC) forms a reverse micelle and then the water/molar ratio is increased to form an anisotropic structure with a nonspherical shape.

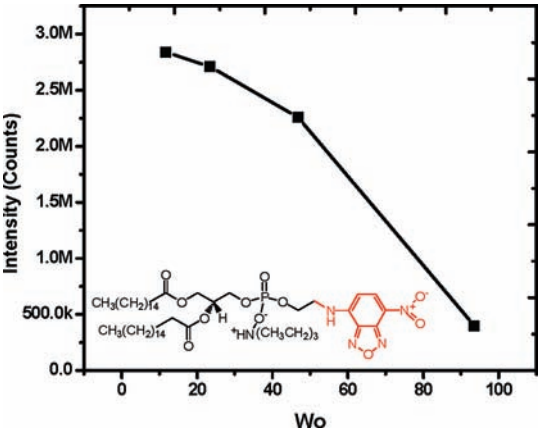

Figure 9. Fluorescence intensity of *N*-(7-nitrobenz-2-oxa-1,3-diazol-4-yl)-1,2-dihexadecanoyl-*sn*-glycero-3-phosphoethanolamine, triethylammonium salt (NBD-PE), in stripped soybean oil with different water/1,2-dioleoyl-*sn*-glycero-3-phosphocholine molar ratios (W_0). The inset is the molecular structure of (NBD-PE).

interface (*19*). The probe is useful because its fluorescence decreases when it is exposed to water. **Figure 9** shows the fluorescence intensity of NBD-PE decreased with increasing water concentrations, suggesting that the exposure of the probe to water increased. The exposure of the probe to the water phase can also be confirmed by a change in the wavelength of maximum fluorescence intensity of NBD-PE, with a red shift occurring when the probe is exposed to a more polar environment (*19*). A red shift of 4 nm was observed for NBD-PE in the DOPC/SSO system when the W_0 was increased from 11.7 to 46.8.

Oxidation of Stripped Soybean Oil Containing Association Colloids. Studies of lipid oxidation in bulk oils have been carried out for several decades, but many of the mechanisms involved in this reaction are still unclear, including whether physical structures in the oil can affect oxidation kinetics. The ultimate purpose of these experiments was to produce soybean oil, water, and phospholipid systems with different physical structures and determine if these physical structures affect lipid oxidation kinetics. Therefore, the lipid oxidation kinetics of SSO containing 1000 μM DOPC or DC_4PC and ~200 ppm water was studied as determined by lipid hydroperoxides and propanal during storage at 37 °C (**Figure 10**). In the presence of DOPC, the lag phases of lipid hydroperoxides (**Figure 10A**) and headspace propanal (**Figure 10B**) were 8 and 13 days, respectively,

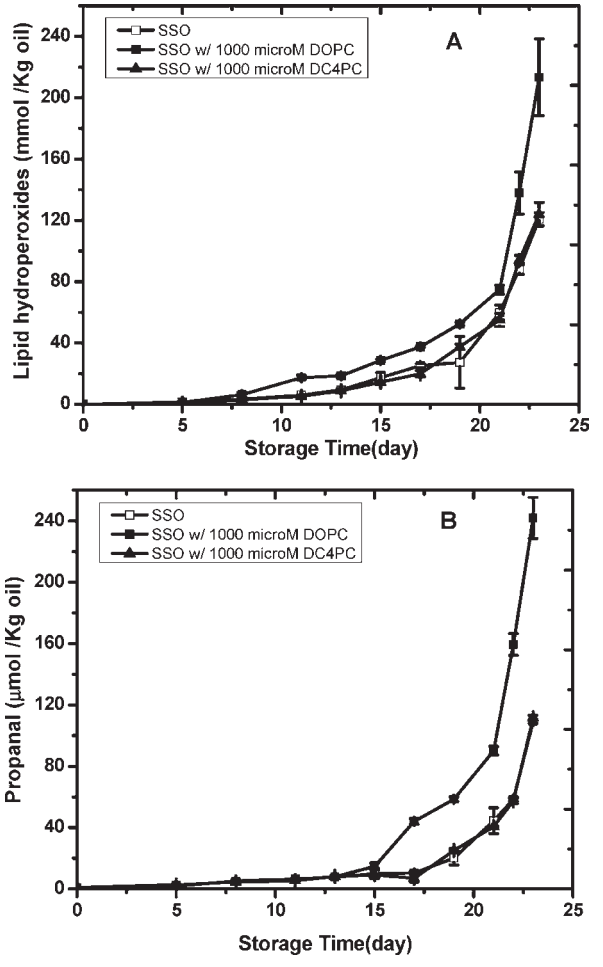

Figure 10. Formation of lipid hydroperoxides (**A**) and propanal (**B**) in stripped soybean oil containing 1000 μM 1,2-dioleoyl-*sn*-glycero-3-phosphocholine (DOPC) or 1,2-dibutyryl-*sn*-glycero-3-phosphocholine (DC_4PC) and 200 ppm water at 37 °C. Data represent means (n = 3) ± standard deviations. Some error bars are within data points.

compared to 13 and 17 days, respectively, for the no-phospholipid control. DC_4PC had the same lag phase times for lipid hydroperoxides and headspace propanal as the control (**Figure 10**).

Phospholipids have previously been reported to have protective effects in bulk oils. The mechanisms for these protective effects have

been postulated to be due to the phospholipid's ability to chelate metals, decompose lipid hydroperoxides, directly scavenge free radicals, and increase the antioxidant activity of tocopherols (*36*). In this study, DOPC and DC_4PC were chosen because they both have identical choline headgroups, so any impact of the phospholipids on alteration in lipid oxidation kinetics by chemical pathways would be similar. Therefore, the major differences in the oil systems containing DOPC and DC_4PC would be in how these phospholipids produced different physical structures. As discussed above, 7,7,8,8-TCNQ was an effective tool to monitor the formation of structures by DOPC, but this probe did not detect structures formed by DC_4PC. Using SAXS, structures could be seen for both DOPC and DC_4PC, but these structures were very different, with DOPC forming spherical and DC_4PC forming cylindrical structures (**Figure 6**). Therefore, these results suggested that the spherical structures formed by DOPC were pro-oxidative, whereas the cylindrical structures formed by DC_4PC had no impact on oxidation rates. These results suggest that phospholipids have the ability to form colloidal structures in vegetable oils and that these structures could have an impact on the oxidative stability of food oils.

ACKNOWLEDGMENT

We greatly thank Dr. Judith Hadley of Agilent Technologies Inc. for loan of the Agilent 7010 particle size spectrophotometer instrument and useful advice and discussions.

LITERATURE CITED

(1) Chaiyasit, W.; Elias, R.; McClements, D. J.; Decker, E. Role of physical structures in bulk oils on lipid oxidation. *Crit. Rev. Food Sci. Nutr.* **2007**, *47* (3), 299−317.

(2) Chaiyasit, W.; Stanley, C. B.; Strey, H. H.; McClements, D. J.; Decker, E. A. Impact of surface active compounds on iron catalyzed oxidation of methyl linolenate in AOT−water−hexadecane systems. *Food Biophys.* **2007**, *2* (2), 57−66.

(3) Xenakis, A.; Papadimitriou, V.; Sotiroudis, T. G. Colloidal structures in natural oils. *Curr. Opin. Colloid Interface Sci.* **2010**, *15* (1−2), 55−60.

(4) Srisiri, W.; Benedicto, A.; O'Brien, D. F.; Trouard, T. P.; Oradd, G.; Persson, S.; Lindblom, G. Stabilization of a bicontinuous cubic phase from polymerizable monoacylglycerol and diacylglycerol. *Langmuir* **1998**, *14* (7), 1921−1926.

(5) Lutton, E. S. Phase behavior of aqueous systems of monoglycerides. *J. Am. Oil Chem. Soc.* **1965**, *42* (12), 1068−1070.

(6) Monduzzi, M.; Ljusberg-Wahren, H.; Larsson, K. R. A C-13 NMR study of aqueous dispersions of reversed lipid phases. *Langmuir* **2000**, *16* (19), 7355−7358.

(7) Ichikawa, S.; Sugiura, S.; Nakajima, M.; Sano, Y.; Seki, M.; Furusaki, S. Formation of biocompatible reversed micellar systems using phospholipids. *Biochem. Eng. J.* **2000**, *6* (3), 193−199.

(8) Abraham, S.; Narine, S. S. Self-assembled nanostructures of oleic acid and their capacity for encapsulation and controlled delivery of nutrients. *J. Nanosci. Nanotechnol.* **2009**, *9* (11), 6326−6334.

(9) Kasaikina, O. T.; Kortenska, V. D.; Kartasheva, Z. S.; Kuznetsova, G. M.; Maximova, T. V.; Sirota, T. V.; Yanishlieva, N. V. Hydrocarbon and lipid oxidation in micro heterogeneous systems formed by surfactants or nanodispersed Al_2O_3, SiO_2 and TiO_2. *Colloid Surface A* **1999**, *149* (1−3), 29−38.

(10) Frankel, E. N. *Lipid Oxidation*; Oily Press: Dundee, Scotland, 1998.

(11) Huang, S. W.; Hopia, A.; Schwarz, K.; Frankel, E. N.; German, J. B. Antioxidant activity of a-tocopherol and Trolox in different lipid substrates: bulk oils vs oil-in-water emulsions. *J. Agric. Food Chem.* **1996**, *44* (2), 444−452.

(12) Boon, C. S.; Xu, Z.; Yue, X.; McClements, D. J.; Weiss, J.; Decker, E. A. Factors affecting lycopene oxidation in oil-in-water emulsions. *J. Agric. Food Chem.* **2008**, *56* (4), 1408−1414.

(13) Wang, Y. H.; Mai, Q. Y.; Qin, X. L.; Yang, B.; Wang, Z. L.; Chen, H. T. Establishment of an evaluation model for human milk fat substitutes *J. Agric. Food Chem. 58* (1), 642−649.

(14) Felgner, A.; Schlink, R.; Kirschenbuhler, P.; Faas, B.; Isengard, H. D. Automated Karl Fischer titration for liquid samples water determination in edible oils. *Food Chem.* **2008**, *106* (4), 1379−1384.

(15) Kanamoto, R.; Wada, Y.; Miyajima, G.; Kito, M. Phospholipid−phospholipid interaction in soybean oil. *J. Am. Oil Chem. Soc.* **1981**, *58* (12), 1050−1053.

(16) Semenyuk, A. V.; Svergun, D. I. GNOM − a program package for small-angle scattering data processing. *J. Appl. Crystallogr.* **1991**, *24* (5), 537−540.

(17) Svergun, D. I. Mathematical methods in small-angle scattering data analysis. *J. Appl. Crystallogr.* **1991**, *24* (5), 485−492.

(18) Svergun, D. I. Determination of the regularization parameter in indirect-transform methods using perceptual criteria. *J. Appl. Crystallogr.* **1992**, *25* (4), 495−503.

(19) Chattopadhyay, A.; Mukherjee, S.; Raghuraman, H. Reverse micellar organization and dynamics: a wavelength-selective fluorescence approach. *J. Phys. Chem. B* **2002**, *106* (50), 13002−13009.

(20) Shantha, N. C.; Decker, E. A. Rapid, sensitive, iron-based spectrophotometric methods for determination of peroxide values of food lipids. *J. AOAC Int.* **1994**, *77* (2), 421−424.

(21) Waraho, T.; Cardenia, V.; Rodriguez-Estrada, M. T.; McClements, D. J.; Decker, E. A. Prooxidant mechanisms of free fatty acids in stripped soybean oil-in-water emulsions. *J. Agric. Food Chem.* **2009**, *57* (15), 7112−7117.

(22) Tarver, T. Food nanotechnology. *Food Technol.* **2006**, *60* (11), 22−26.

(23) Papadimitriou, V.; Pispas, S.; Syriou, S.; Pournara, A.; Zournpanioti, M.; Sotiroudis, T. G.; Xenakis, A. Biocompatible microemulsions based on limonene: formulation, structure, and applications. *Langmuir* **2008**, *24* (7), 3380−3386.

(24) Zhang, S. Fabrication of novel biomaterials through molecular self-assembly. *Nat. Biotechnol.* **2003**, *21* (10), 1171−1178.

(25) King, M. D.; Marsh, D. Head group and chain length dependence of phospholipid self-assembly studied by spin-label electron spin resonance. *Biochemistry* **1987**, *26* (5), 1224.

(26) Shiao, S. Y.; Chhabra, V.; Patist, A.; Free, M. L.; Huibers, P. D. T.; Gregory, A.; Patel, S.; Shah, D. O. Chain length compatibility effects in mixed surfactant systems for technological applications. *Adv. Colloid Interface Sci.* **1998**, *74*, 1−29.

(27) Ali, N.; Sul, W. H.; Lee, D. Y.; Kim, D. H.; Park, S. Y. Structures of the cylindrical and vesicular micelles of an P4VP-longer asymmetric PS-b-P4VP. *Macromol. Res.* **2009**, *17* (8), 553−556.

(28) Chaiyasit, W.; McClements, D. J.; Weiss, J.; Decker, E. A. Impact of surface-active compounds on physicochemical and oxidative properties of edible oil. *J. Agric. Food Chem.* **2008**, *56* (2), 550−556.

(29) Eicke, H. F.; Christen, H. Is water critical to the formation of micelles in apolar media? *Helv. Chim. Acta* **1978**, *61* (6), 2258−2263.

(30) Tung, S. H.; Huang, Y. E.; Raghavan, S. R. A new reverse wormlike micellar system: mixtures of bile salt and lecithin in organic liquids. *J. Am. Chem. Soc.* **2006**, *128* (17), 5751−5756.

(31) Langevin, D. Micelles and microemulsions. *Annu. Rev. Phys. Chem.* **1992**, *43* (1), 341−369.

(32) Ohshima, A.; Narita, H.; Kito, M. Phospholipid reverse micelles as a milieu of an enzyme reaction in an apolar system. *J. Biochem.* **1983**, *93* (5), 1421.

(33) Gochman-Hecht, H.; Bianco-Peled, H. Structure of AOT reverse micelles under shear. *J. Colloid Interface Sci.* **2005**, *288* (1), 230−237.

(34) Mezzasalma, S. A.; Koper, G. J. M.; Shchipunov, Y. A. Lecithin organogel as a binary blend of monodisperse polymer-like micelles. *Langmuir* **2000**, *16* (26), 10564−10565.

(35) Gupta, R.; Muralidhara, H. S.; Davis, H. T. Structure and phase behavior of phospholipid-based micelles in nonaqueous media. *Langmuir* **2001**, *17* (17), 5176−5183.

(36) Koga, T.; Terao, J. Phospholipids increase radical-scavenging activity of vitamin-E in a bulk oil model system. *J. Agric. Food Chem.* **1995**, *43* (6), 1450−1454.

Received for review July 16, 2010. Revised manuscript received September 20, 2010. Accepted October 4, 2010. This material is based upon work supported by the U.S. Department of Agriculture (Project 2007-02650).